Nanoscale

RSC Publishing

PAPER

View Article Online
View Journal

Hyaluronan degrading silica nanoparticles for skin cancer therapy†

Cite this: DOI: 10.1039/c3nr02787b

P. Scodeller,*[a] P. N. Catalano,‡[b] N. Salguero,‡[b] H. Duran,[b] A. Wolosiuk[a] and G. J. A. A. Soler-Illia[a]

We report the first nanoformulation of Hyaluronidase (Hyal) and its enhanced adjuvant effect over the free enzyme. Hyaluronic acid (HA) degrading enzyme Hyal was immobilized on 250 nm silica nanoparticles (SiNP) maintaining specific activity of the enzyme *via* the layer-by-layer self-assembly technique. This process was characterized by dynamic light scattering (DLS), zeta potential, infrared and UV-Vis spectroscopy, transmission electron microscopy (TEM) and enzymatic activity measurements. The nanoparticles were tested *in vivo* as adjuvants of carboplatin (CP), peritumorally injected in A375 human melanoma bearing mice and compared with the non-immobilized enzyme, on the basis of equal enzymatic activity. Alcian Blue staining of A375 tumors indicated large overexpression of hyaluronan. At the end of the experiment, tumor volume reduction with SiNP-immobilized Hyal was significantly enhanced compared to non-immobilized Hyal. Field emission scanning electron microscopy (FE-SEM) images together with energy dispersive X-ray spectroscopy (EDS) spectra confirmed the presence of SiNP on the tumor. We mean a proof of concept: this extracellular matrix (ECM) degrading enzyme, immobilized on SiNP, is a more effective local adjuvant of cancer drugs than the non-immobilized enzyme. This could prove useful in future therapies using other or a combination of ECM degrading enzymes.

Received 29th May 2013
Accepted 30th July 2013

DOI: 10.1039/c3nr02787b

www.rsc.org/nanoscale

Published on 01 August 2013. Downloaded by Open University on 23/08/2013 18:58:47.

1 Introduction

The ability of an oncolytic drug to reach a solid tumor is hampered by the overexpression of Hyaluronic Acid (HA) that occurs in many tumors.[1] This has been demonstrated by comparing drug concentration profiles in tumors with and without prior peritumoral treatment with the HA-degrading enzyme Hyaluronidase (Hyal).[2,3] HA is overexpressed in cancer[4] to an extent that varies with the type of tumor and has been recently quantitatively compared to normal tissue for many different tumors.[5] The overexpression of HA results in a gel-like extracellular matrix which resists the penetration of external fluid and drugs dissolved therein, and elevates the *interstitial fluid pressure* (IFP), the physical parameter as measured using the wick-in-needle method[6,7] or the parameter as measured by Hingorani *et al.*[8]

Hyal (EC 3.2.1.35 – hyaluronoglucosaminidase) is a 60 kDa, ~6 nm in diameter tetramer that catalyzes the hydrolysis of the $\beta_{1\rightarrow4}$ glycosidic bond in HA and chondroitin sulfate,[9] thus breaking up these megadalton polymers into smaller constituents and oligosaccharides.[10–12] Subcutaneous use of Hyal derived from crude extracts of ovine or bovine testicular tissue was approved by the FDA in 1948 (ref. 13) for treatments like hypodermoclysis and as an adjunct in subcutaneous urography and treatment of vitreous hemorrhage.[14] In cancer,[15] there are ongoing clinical trials with intravenous application of a *PEGylated*, recombinant human Hyal (PEGPH20) as a chemoadjuvant for advanced solid tumors and pancreatic cancer.[16]

When Hyal is administered to tumors, subcutaneously or intravenously, it degrades HA into smaller molecular weight fragments and lowers the IFP.[17,18] The enhancement in drug penetration with the enzymatic pretreatment is attributed to this IFP-lowering power of Hyal. The localized subcutaneous pretreatment with Hyal is preferred – over the systemic route – for being clinically approved[1] and not having side effects (the heart and bowels contain modest amounts of HA and systemic administration of Hyal was shown to degrade it[18]).

In subcutaneous tumors, numerous reports showed an improved cancer therapy with *peri-* or *intra*-tumoral administration of Hyal, acting as an adjuvant of oncolytic drugs,[19] nanoformulated drugs,[2] and oncolytic viruses[20–22] and radioimmunotherapy.[23] However, in all of those cases, the enzyme is administered in free form. Functionalized silica nanoparticles are a very promising tool for cancer therapy.[24,25] In this work we

[a]*Gerencia de Química, Comisión Nacional de Energía Atómica (CNEA), Av. Gral. Paz 1499, (B1650KNA) San Martín, Argentina. E-mail: pscodeller@sanfordburnham.org*

[b]*Laboratorio de Aplicaciones Biológicas, Departamento de Micro y Nanotecnología, Comisión Nacional de Energía Atómica (CNEA), Av. Gral. Paz 1499, (B1650KNA) San Martín, Argentina*

† Electronic supplementary information (ESI) available. See DOI: 10.1039/c3nr02787b

‡ These authors contributed equally.

Published on 01 August 2013. Downloaded by Open University on 23/08/2013 18:58:47.

report on the first nanoformulation of Hyal as chemotherapy adjuvant, immobilized on 250 nm silica nanoparticles and show that this configuration is more effective than using the free enzyme.

We hypothesized that Hyal, while bigger and heavier than any oncolytic drug, would also suffer from the deleterious effect of IFP and that nanocarrier-immobilized Hyal would be retained on the tumor (the site of injection) more than free Hyal, thanks to: (A) larger molecular weight of SiNP and hence smaller diffusion coefficient; and (B) adsorption of Hyal-carrying particles on the tumor since nanostructures provide multivalent interactions with a target and hence a larger affinity. Moreover, HA is very rapidly turned over in the human body[26] and so a tumor-dwelling Hyal that prevents HA regeneration would be very attractive.

In summary, this paper reports two findings: (1) the first active immobilization of Hyal onto colloidal surfaces and (2) a new nanoformulation of Hyal which enhances the therapeutic outcome as compared to the free adjuvant, and is a proof of concept for future therapies involving this or other ECM-degrading enzymes used as adjuvants of oncolytic agents.

2 Results and discussion

Hyal can be adsorbed on SiNP maintaining stability in PBS and enzymatic activity

Silica nanoparticles synthesized by the well-known Stöber method[27] were chosen for this study since they are reproducibly and inexpensively fabricated, monodisperse, electrically charged and have been shown to be non-toxic at concentrations of up to 1 mg SiO_2 mL^{-1}.[25,28,29] In this work, particles measured 250 nm in diameter by TEM and DLS (Fig. S1† and 2A respectively) and showed a zeta potential of −43 mV (Fig. 2A). To functionalize these particles with Hyal we used the layer-by-layer (LBL) self-assembly technique,[30] which consists of the alternate adsorption of polycations and polyanions from water solutions, where each layer deposition is accompanied by charge reversal as a result of charge overcompensation.[31] This technique is the most appealing when functionalizing surfaces with enzymes since enzymatic activity is maintained and multiple layers may be deposited to yield a larger response; this method has been successfully employed to construct catalytically active enzymatic multilayers by self-assembling enzymes and polymers on planar[32] and colloidal surfaces.[33] The catalytic activity of this multilayer will depend on enzymatic loading, enzyme orientation and mobility, parameters which are directly controlled by the deposition conditions (assembly pH and ionic strength).[34] Since Hyal reports a pI of 5.1–6,[35] it is expected to bear a slight net negative charge in our deposition conditions (water pH), so we deposited a sacrificial – positive – layer of polyallylamine as shown in the schematic diagram of Fig. 1.

The two features shown in Fig. 2A, namely charge reversal and increasing particle diameter with the number of layers, are characteristic of this LBL on colloids process.[36] Also, the appearance of peaks at 1543 cm^{-1} and 1655 cm^{-1} in the IR spectrum of SiNP/PAH/Hyal (Fig. 2B), assignable to Amide I and Amide II bands respectively, indicates adsorption of protein in the last deposition step. Fig. 1B shows a typical TEM image of SiNP/PAH/Hyal particles, confirming the core–shell structure, with a visible shell measuring approximately 6 nm in thickness in this dry state (Fig. S2† shows another picture of these particles); Fig. 1C shows an image of the same TEM grid inspected by FE-SEM and the EDS spectrum of this sample in panel 1D confirms the presence of silicon.

Since SiNP/PAH/Hyal were to be used in PBS, DLS and zeta-potential measurements of these particles were carried out in that buffer. Under these conditions, the particles were negative (−12.4 mV) and DLS indicated a diameter of 520 nm. This apparent hydrodynamic radius is expected as the ionic strength of the buffer is relatively high. As already observed by Schärtl,[37] depending on colloidal particle interactions, apparent diffusion coefficients predicted by the Stokes–Einstein equation may strongly deviate from the observed value which determines the particle size (see details in Fig. S5†). Nonetheless, the modified SiO_2 particles sedimented after a couple of days, pointing to the fact that there was no physical aggregation. In addition, we could observe individual particles on the TEM grid even after solvent evaporation (Fig. 1A).

The amount of protein on the nanoparticles was estimated from the difference in the UV-Vis spectra, at 280 nm, of Hyal functionalized particles and non-functionalized particles, as described in Section 3 of the ESI.† Enzymatic activity of Hyal was quantified using the standard turbidimetric assay. Under the conditions of this assay high molecular weight HA forms cloudy precipitates when incubated with bovine serum albumin, while HA fragments produced by the enzymatic cleavage do not (see "*Enzymatic activity of Hyal and SiNP/PAH/Hyal*" in Section 5). Solutions of free Hyal at the same concentration presented the same enzymatic activity suggesting that the specific activity of Hyal (defined as enzymatic activity per mg of protein) was maintained when the enzyme was immobilized on these particles under these conditions. In the only previous report of Hyal immobilization that we know of, on a planar macroscopic surface,[38] researchers suggested that the active binding of Hyal required hydrophobic binding surfaces in order to expose the hydrophilic active site of the enzyme to the solution. In this work, when a SiNP/PAH solution with a pH of 6.5 or below instead of 9 was used to self-assemble Hyal, no enzymatic activity was observed, suggesting that less charged surfaces (and perhaps also hydrophobic interactions) are needed to adsorb Hyal in a catalytically active manner.

SiNP/PAH/Hyal particles that were kept at room temperature for ten days showed 90% of the initial activity; the same happened with free Hyal solutions. Importantly, no enzymatic activity was observed with SiNP/PAH particles or with SiNP alone, suggesting that no adsorption or degradation of HA occurs under the conditions of the enzymatic assay that might generate a false positive activity reading. Ten days after fabrication, the core–shell particles centrifuged and separated from the supernatant showed 90% of initial activity, suggesting no desorption of the catalytically active multilayer from the particles.

This represents the first novelty of this paper: the successful immobilization of an ECM degrading enzyme with pharmaceutical applications on the surface of nanoparticles. We have shown

 This journal is © The Royal Society of Chemistry 2013

Published on 01 August 2013. Downloaded by Open University on 23/08/2013 18:58:47.

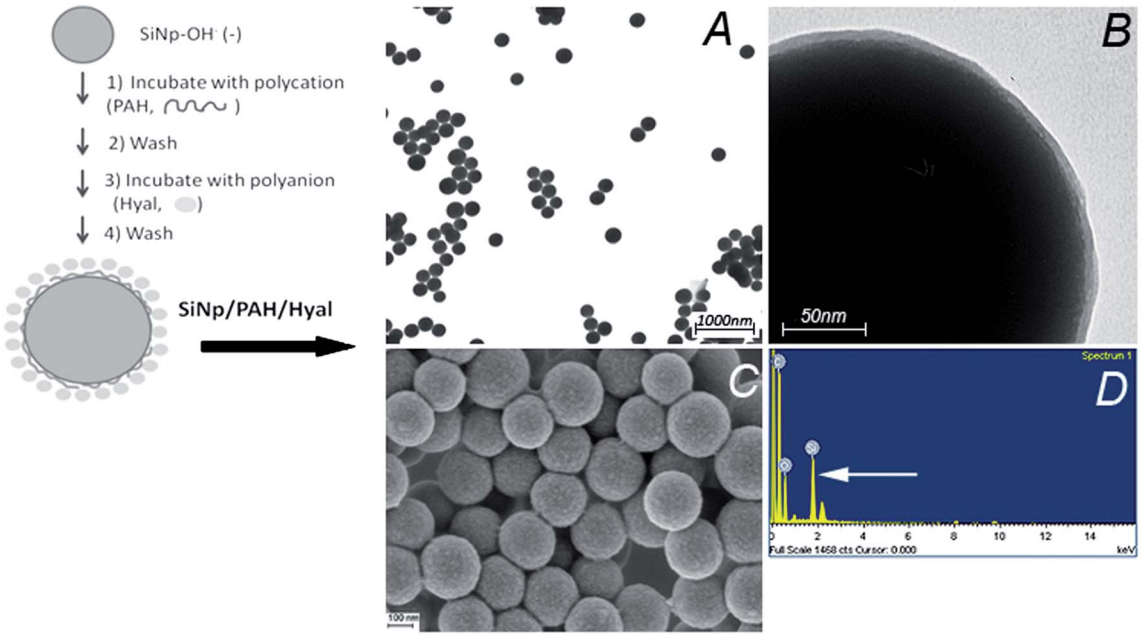

Fig. 1 Left: schematic depiction of the layer-by-layer self-assembly of the polymer and enzyme on SiNP to obtain the core–shell nanoparticles. Panels A and B show transmission electron microscopy (TEM) images of core–shell SiNP/PAH/Hyal particles; (A) collection of these particles as deposited on the copper grid; (B) closeup view on one particle, showing the core material (SiO_2) and the soft matter shell (polyelectrolyte). Panel C shows a typical scanning electron microscopy image of the metallized SiNP/PAH/Hyal particles deposited on a formvar coated TEM grid, and panel D displays the corresponding EDS spectra showing the Si peak highlighted by the arrow.

that SiNP/PAH/Hyal particles are stable in physiological buffer and are active *in vitro*. This is the first report in the literature of catalytically active immobilized Hyal on a colloidal surface.

Alcian Blue staining shows large content of glycosaminoglicans in A375 tumors

To confirm that A375 tumors indeed overexpress HA, we stained tumor slides with Alcian Blue. This dye binds acidic polysaccharides such as glycosaminoglycans and is one of the procedures used to stain hyaluronic acid.[18,20,35,39] Acid mucopolysaccharides stained by the Alcian Blue technique show up light blue-turquoise under the optical microscope.

Fig. 3A shows a typical image of Alcian Blue stained sections of A375 tumors used in this study. Panel B is the image that serves as a control for the staining method (human colon cells, which produce large amounts of mucopolysaccharides).

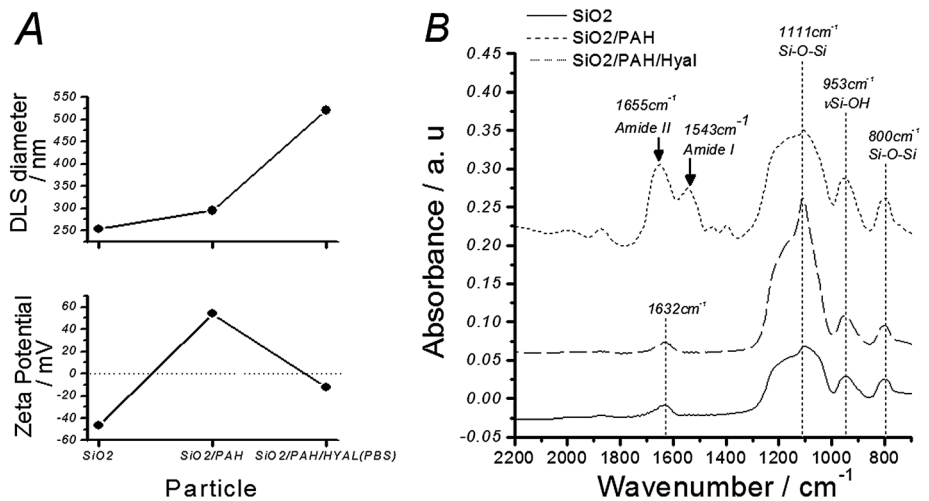

Fig. 2 (A) DLS diameter and zeta-potential of the particles after each deposition step (lines connecting the dots are a visual guide). (B) DRIFTS infrared spectroscopy of the particles after each deposition step, showing the characteristic SiO_2 features of SiNP (1111 cm^{-1}: Si–O–Si; 953 cm^{-1}: νSi–OH; 800 cm^{-1} Si–O–Si) (solid line), and the Amide I (1543 cm^{-1}) and Amide II (1655 cm^{-1}) band for the enzyme functionalized particles (dotted line). The spectra of panel B were arbitrarily displaced in the *Y*-direction for more clarity.

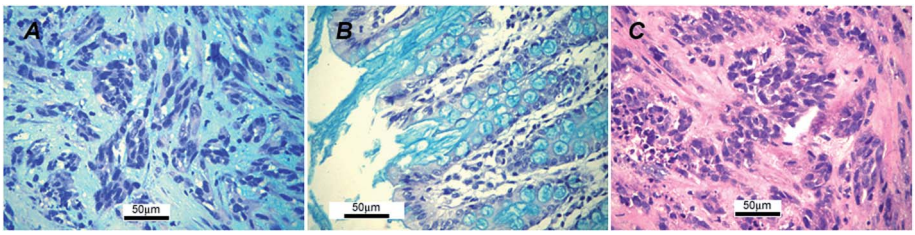

Fig. 3 Typical images of Alcian Blue (A) and H&E (C) stained A375 tumor slides. (B) Human colon control for Alcian Blue. In A and B, light blue-turquoise indicates staining of acid mucopolysaccharides and blue-purple indicates staining of nuclei.

Published on 01 August 2013. Downloaded by Open University on 23/08/2013 18:58:47.

Panel C (Hematoxylin and Eosin, H&E, of an A375 tumor) shows the large ECM content of this tissue, while Fig. 3A confirms the presence of acidic polysaccharides, like HA, in that ECM.

Adjuvant effect of Hyal is enhanced when immobilized on nanoparticles

In view of the *in vitro* activity of Hyal derivatized nanoparticles and the overexpression of HA observed in A375 tumors, we performed an animal study to assess the adjuvancy power of these nanostructures as spreading factors for carboplatin.

Carboplatin is a small (371 Da) water soluble drug, used in this study as the therapeutic agent. Groups receiving the adjuvant, in free or immobilized form, were given 20 U of the enzyme, an activity similar to the one used in previous reports.[1] By "treatment groups" we denoted all groups that received at least the oncolytic drug, namely: CP, Hyal/CP and NP/CP (see Table 1, Experimental section).

The left panel of Fig. 4A shows the three treatment groups compared to the PBS control group, where treatment days are indicated by arrows. Treatment was started when tumors were 70 mm^3. While tumors were sensitive to the drug alone, these showed a stable growth and tumor shrinkage never occurred throughout the treatment; the average tumor volume at the end of the experiment was 176 mm^3 (Fig. 4B). The group receiving free enzyme pretreatment (Hyal/CP) showed a slower growth than the CP group but hardly any tumor shrinkage was observed during the treatment and the final tumors measured 105 mm^3 (Fig. 4B). On the other hand, with NP/CP, a stark tumor shrinkage was observed during the first days of treatment, until day 42 when the mean volume size dropped to a minimum of 19.5 mm^3 (from the initial 70 mm^3). Moreover, when the last treatment was applied on day 65, only the NP/CP group responded in terms of volume change (−25%), while Hyal/CP

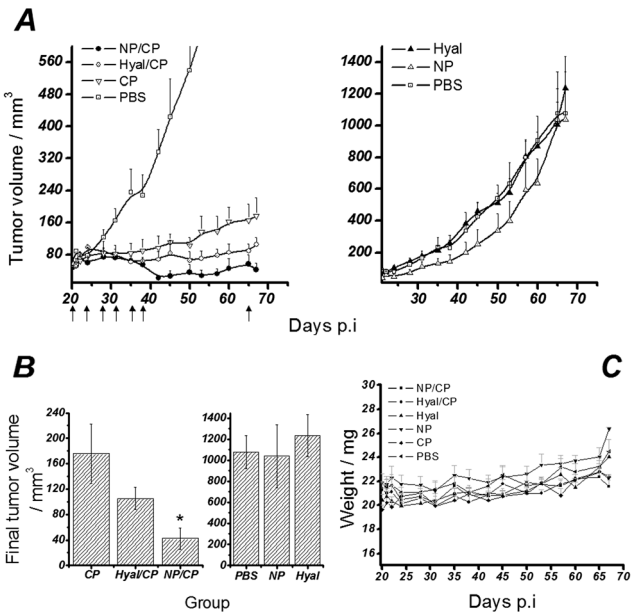

Fig. 4 (A) A375 tumor volume curves for the six groups ($n = 5$) as a function of post-injection (p.i.) day. For the sake of clarity, the groups are shown in separated panels: left: treated groups (NP/CP, CP, Hyal/CP) and PBS control, right: all control groups. Treatment days are indicated by arrows. (B) Final tumor volumes for all treated groups. (C) Body weight of all groups during the experiment.

and CP showed increases (+17% and +7% respectively). End value tumor volume differences between the NP/CP group and the Hyal/CP group were statistically significant ($p < 0.05$) (Fig. 4B).

To discard a therapeutic effect of the NP alone, one group was injected solely with NP (right panel of Fig. 4A). This group showed no significant differences in tumor growth kinetics compared to the PBS group and the Hyal group.

Table 1 Injections carried out for the different groups in the animal experiment

Group	First injection	Second injection (two hours later)
(1) PBS ("PBS")	0.1 mL PBS	0.1 mL PBS
(2) Core shell SiNP ("NP")	SiNP/PAH/Hyal (0.1 mL, 0.5 mg mL^{-1})	0.1 mL PBS
(3) Hyal ("Hyal")	Hyal (0.1 mL in PBS, 20 U)	0.1 mL PBS
(4) Drug ("CP")	Carboplatin (0.1 mL, 3 mg mL^{-1} diluted in PBS)	0.1 mL PBS
(5) Free adjuvant ("Hyal/CP")	Hyal (0.1 mL in PBS, 20 U)	Carboplatin (0.1 mL, 3 mg mL^{-1} diluted in PBS)
(6) Immobilized adjuvant ("NP/CP")	NP (0.1 mL, 0.5 mg mL^{-1})	Carboplatin (0.1 mL, 3 mg mL^{-1} diluted in PBS)

This journal is © The Royal Society of Chemistry 2013

Published on 01 August 2013. Downloaded by Open University on 23/08/2013 18:58:47.

No significant body weight loss was observed in all the treated mice in comparison with the control mice group (Fig. 4C). Throughout the experiment, no mouse showed toxicity, defined by shivering, inactivity, severe necrosis, ataxic gait, extreme weakness or weight loss exceeding 20% of the initial weight.

This represents the second finding of this work: the enhanced therapeutic effect of these catalytically active nanoparticles when used as an adjuvant of carboplatin, with respect to free Hyal, in mice carrying A375 tumors.

To further investigate the distribution of NPs at the tumor site, we performed FE-SEM analysis (Fig. 5) of the surfaces of NP-injected tumors (panel A) and PBS-injected tumors (panel B). The spheres seen in Fig. 5A are identical to the ones in Fig. 1C and measure 250 nm in diameter (see Fig. S8 of ESI†); furthermore, elemental analysis of this sample with EDS revealed a clear silicon peak. On the other hand, PBS-injected tumor (Fig. 5B) showed no such particles and no silicon peak. These images confirm the presence of the NPs in the tumor, and suggest the affinity of these towards the tissue, as they remained in the site even after the thorough washing processes this sample preparation demanded. A larger affinity of the particles for tumor tissue might be another reason to explain the enhanced adjuvant effect: it would translate into a longer Hyal residence time in the tumor preventing the regeneration of HA, which normally undergoes a very rapid turnover rate.[26] These FE-SEM images, together with the fact that the particles are still catalytically active ten days after, suggest that using a single shot of this adjuvant throughout the treatment might be just as effective.

To explain the enhanced adjuvant effect of Hyal when immobilized on a nanostructure we suggest the mechanism illustrated in Fig. 6. Hyaluronidase, while larger than oncolytic drugs, would also suffer from the IFP effect. On the other hand,

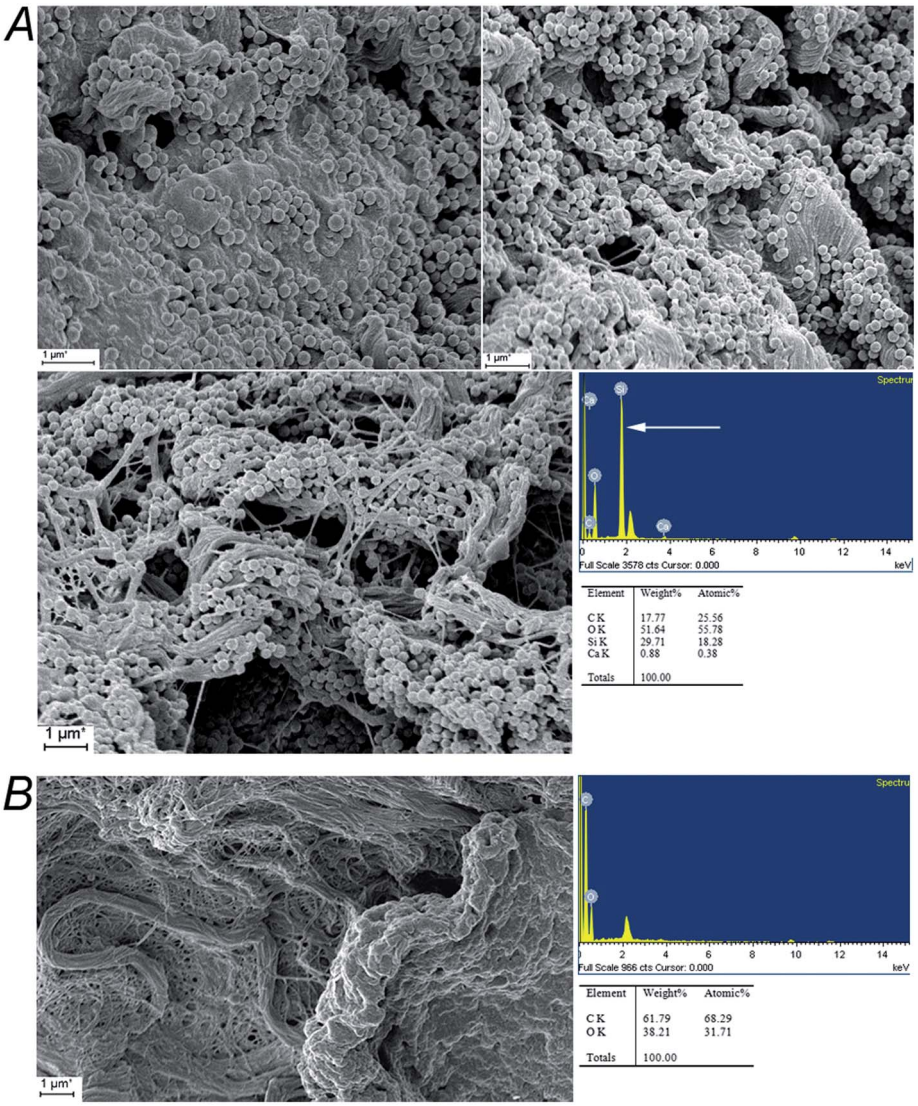

Fig. 5 Surface of A375 tumors as seen with FE-SEM, 21 days after injection of cells. (A) Two hours after one injection of core–shell particles and the EDS spectrum for that sample showing the presence of silicon (the arrow marks the silicon peak). (B) Two hours after one injection of PBS and the corresponding EDS spectrum showing no presence of silicon.

Published on 01 August 2013. Downloaded by Open University on 23/08/2013 18:58:47.

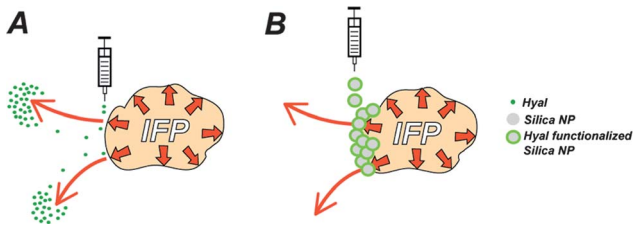

Fig. 6 Proposed mechanism to explain the enhanced adjuvant effect of Hyal when immobilized on a nanostructure. (A) Free Hyal. (B) Immobilized Hyal. Hyal, while larger than oncolytic drugs, also suffers from the IFP effect. On the other hand, large Hyal-carrying nanoparticles are expected to be retained where they are injected (at the tumor site), as a consequence of the combination of: (1) a larger molecular weight and hence smaller diffusion coefficient and (2) adsorption of the nanostructures on the tumor (multivalent interactions of nanostructures with the tumor tissue generate larger affinity compared to one molecule of free Hyal).

large Hyal-carrying nanoparticles are expected to be retained where they are injected (in this case the tumor exterior), as a result of the combination of: (1) a larger molecular weight and hence smaller diffusion coefficient, and (2) adsorption of the nanostructures on the tumor (multivalent interactions of nanostructures with the tumor tissue generate larger affinity as compared to one molecule of free Hyal).

3 Conclusion

We have assayed a new local adjuvant of carboplatin in melanoma and proved the concept that hyaluronidase, an ECM-degrading enzyme, when immobilized on nanoparticles, is a better local chemoadjuvant than the non-immobilized enzyme. The layer-by-layer technique proved to be an effective way to immobilize colloidal surfaces with hyaluronidase in a stable and catalytically active configuration. In addition, only subcutaneous use of Hyal is FDA approved and hence our system is clinically relevant.

Improvements to our system might arise from using: (A) Mesoporous Silica Nanoparticles (MSNs), instead of Stöber particles, to entrap a cancer drug or a photosensitizer[24] (it was shown that MSNs release drugs from the pores even in the presence of a polymeric coating of the MSNs' surface[25,40,41]) and (B) multiple ECM degrading enzymes, like macrophage metalloelastase, elastase or relaxin.[22]

We also envision the peritumoral injection of hyaluronidase functionalized particles to identified primary tumors like pancreatic (by ultrasound guided injection), a very aggressive type of tumor known to be particularly rich in hyaluronan.[42]

4 Experimental section

Synthesis of silica nanoparticles

Silica nanoparticles were prepared according to the well established Stöber synthesis.[27] In this paper, "water" will denote water of MilliQ grade (18.2 MΩ). Glass material was washed with alcoholic potassium hydroxide and rinsed with water. To prepare 250 nm particles, NH_3 (30%, 2 mL), absolute ethanol (48.75 g) and water (13.13 mL) were mixed and stirred vigorously. Then tetraethoxysilane (TEOS, 3.04 mL) was added at once, with a syringe, at the vortex of the solution. Half an hour later the solution started to turn white; stirring was continued for 24 hours, after which the particles were washed to remove ammonia with 10 centrifugation cycles of 20 min at 7000 × *g* and resuspended in water. The synthesis was carried out at room temperature. The resulting particles were characterized by TEM, UV-Vis and IR spectroscopy and DLS and zeta-potential.

Particle concentration throughout the paper is expressed as mg of SiO_2 mL^{-1} and was controlled by weighing and dispersing the air-dried material. The weight of a single 250 nm SiNP, using the density value of bulk silica, is 2.2×10^{-14} g. For the *in vivo* experiments, 0.5 mg mL^{-1} particle concentrations were used, which corresponds to 23×10^9 NP mL^{-1}. No particle loss was detected during the centrifugation cycles.

Synthesis of hyaluronidase functionalized silica nanoparticles

A suspension of SiNP (10 mL of 0.5 mg mL^{-1} in water) was added dropwise, while stirring, to 10 mL of polyallylamine hydrochloride (PAH, Sigma-Aldrich) 1% w/v, pH 9 (pH was adjusted by adding NaOH) in water at room temperature. After 30 min of incubation, the particles were washed to remove the excess of PAH by 3 centrifugation cycles of 1000 × *g* and 30 min, always redispersing the pellet with MilliQ water. Then, 10 mL of these particles were added dropwise to 10 mL of 1 mg mL^{-1} hyaluronidase (Hyal Type IV-S from Bovine Testes, Sigma-Aldrich, 1492 U mg^{-1}) with stirring. After one hour, the particles were washed with three centrifugation cycles of 30 min and 1000 × *g*. In every case the pellets were easily resuspended by hand shaking. After each deposition step particles were characterized by DLS, zeta-potential, TEM and UV-Vis spectroscopy; in addition, SiNP/PAH/Hyal were characterized by FE-SEM.

Nanoparticle characterization

Hydrodynamic radii of particles were measured using Dynamic Light Scattering (DLS) with a Brookhaven BI-200 SM apparatus fitted with an avalanche photodiode detector and a He–Ne laser (wavelength 637 nm). For this, diluted solutions of particles were prepared in water + 10 μM KCl for all samples except the SiNP/PAH/Hyal, which was also measured in Phosphate Buffered Saline (PBS). All samples were measured with the collector placed at a 90° angle from the laser source. The zeta potential was measured with a Malvern Zetasizer 2000 instrument using the same solutions used to measure DLS. Diffuse reflectance infrared Fourier transform spectroscopy (DRIFTS) measurements were performed with a Nicolet Magna 560 instrument, equipped with a liquid nitrogen cooled MCT-A detector, by air drying a small pellet of centrifuged particles. Absorbance was measured using a Hewlett-Packard 8453 spectrophotometer in transmission mode, using 1 cm path length quartz cuvettes. Transmission electron microscopy (TEM) images were taken using a Philips EM 301 transmission electron microscope operated at 60 kV (CMA, Facultad de Ciencias Exactas y Naturales, UBA), these samples were prepared by depositing a drop

 This journal is © The Royal Society of Chemistry 2013

Published on 01 August 2013. Downloaded by Open University on 23/08/2013 18:58:47.

of a very dilute particle dispersion on carbon-coated copper grids and letting it air-dry.

FE-SEM images were taken with a Zeiss Leo 982 Gemini microscope in the secondary-electron mode using an in-lens detector. This microscope is coupled to an Oxford Instruments EDS detector.

Enzymatic activity of Hyal and SiNP/PAH/Hyal

The enzymatic activity of Hyal was measured by the standard turbidimetric enzymatic assay.[43] Hyaluronic acid was purchased from Sigma-Aldrich (hyaluronic acid sodium salt from streptococcus equi). To determine SiNP/PAH/HYAL activity, the particles were previously removed by centrifugation with 1000 × *g* for 2 min (see Section 5 of ESI†). To estimate the protein loading on the particles the peak of 280 nm was used of the UV-Vis spectral difference between Hyal functionalized particles and particles without Hyal (see Section 3 of ESI†). The amount of protein in 100 μL of 0.5 mg mL^{-1} SiNP/PAH/Hyal sample was 15 μg and the enzymatic activity of this sample yielded 20 U. The enzymatic activity of the free enzyme at the same concentration (15 μg, 100 μL^{-1}) yielded the same enzymatic activity. Since 100 μL of total volume were used for the adjuvant injections, the enzymatic activity in each of those vials was 20 U.

Cells and culture

The human, non-metastatic, melanoma cancer cell line A375, kindly provided by Dr Estela Medrano (Huffington Center on Aging, Departments of Molecular & Cellular Biology and Dermatology, Baylor College of Medicine, Houston, TX, USA), was grown in DMEM-F12 (Invitrogen Argentina S.A.) supplemented with fetal calf serum (10%, Natocor, Córdoba, Argentina) ascorbic acid (17.6 μg mL^{-1}), pyruvic acid (150 μg mL^{-1}), galactose (300 μg mL^{-1}), insulin (5 μg mL^{-1}), penicillin (50 U mL^{-1}), and streptomycin (50 μg mL^{-1}) at 37 °C in a 5% CO_2 humidified atmosphere. The medium was routinely changed every 3 days and the cells were diluted by trypsinization before reaching confluency.

Animals

Seven week-old female nude athymic mice (purchased from Bioterio Facultad de Veterinaria, Universidad de La Plata, Argentina) were maintained in disposable plastic cages with hardwood chip bedding in an air-conditioned room with a 12-hour-light–12-hour-dark cycle and given food and filtered tap water ad libitum. All animal experiments were performed following the protocols approved by the CNEA Animal Research committee.

Human cancer xenograph establishment

For xenografts established from cultured cells, 2.5×10^6 A375 cells, collected in PBS, were subcutaneously injected into the right lateral abdominal wall of 30 mice. When tumors reached ≈5 mm in diameter (21 days after inoculation) and ≈70 mm^3, mice were randomly divided into 6 groups of 5 animals each.

Treatments

Thirty mice were randomly subdivided into 6 groups and seven treatments were applied, twice per week, each consisting of 2 peritumoral injections, according to Table 1.

A dose concentration of 15 mg kg^{-1} was used for carboplatin. Based on prior studies of HA degradation with time after local treatment with Hyal,[2,17] and to ensure an optimum degradation of HA at the time of CP injection, the drug was administered two hours after the adjuvant application. To ensure full enzymatic activity, fresh batches of Hyal functionalized particles and free Hyal solution were prepared prior to each treatment.

Tumor volume and body weight were monitored every 3 days. Tumor volume, *v*, was calculated using the formula $v = 1/2$ $(L \times W \times T)$, where *L* is the length, *W* is the width and *T* is the thickness of the tumor respectively, measured with a Vernier caliper. On the final day, all mice were sacrificed and subjected to autopsy; tumors were excised and kept in 4% formaldehyde in PBS buffer for 48 h. The endpoint criterion for the control groups was based on the tumor volume.

Statistical analysis

Data were expressed as mean ± SE. Statistical analysis was performed using Statsoft Statistica 8.0® (Tulsa, OK). Differences between groups were analyzed using repeated measures ANOVA for comparing the tumor volume over the range of days following injection of cells. One way ANOVA was performed on the final tumor volume between groups 4, 5 and 6. A value of $p < 0.05$ was considered significant.

Histology of tissues

For Alcian Blue staining, tumor and human colon sections of 3 μm were deparaffinized and hydrated, mordanted with 3% acetic acid for 10 min, incubated in an Alcian Blue solution of pH 2.5 (AB 1 g in 100 mL of acetic acid 3%) for 30 min, washed with distilled water for 5 minutes, and counterstained with hematoxiline for 10 min, then dehydrated, cleared and mounted. Human colon cells were used as the control for positive Alcian Blue staining since this tissue is known to produce high levels of mucopolysaccharides. Tumor sections were also stained using the standard hematoxiline and eosine protocol and all the images were analyzed with the help of an expert pathologist. Digital images were taken with a Nikon Eclipse E200 Microscope (Nikon Corp., Japan) fitted with a digital still camera (Micrometric SE Premium, Nikon Corp.).

Preparation of tumors for SEM imaging

Two mice were inoculated with 2.5×10^6 A375 cells. After 21 days these mice were peritumorally injected, one with 100 μL of core–shell SiNP, and the other one with 100 μL of PBS. Two hours later, both mice were euthanized and their tumors were excised and fixed in 4% formaldehyde for 2 days. Formaldehyde was gradually displaced with ethanol by immersing the tumors for two hours in ethanol–water solutions of increasing ethanol concentration. The tumors in absolute ethanol were dried using critical point and were metallized for FE-SEM characterization.

Published on 01 August 2013. Downloaded by Open University on 23/08/2013 18:58:47.

Acknowledgements

The authors are grateful to CONICET (PIP 00186), University of Buenos Aires (UBACYT 20020110100081), ANPCyT (PICT 1848 and PAE-37063-PME-2006-00038) and INN-Comision Nacional de Energia Atomica for financial support. P.S. acknowledges a postdoctoral research fellowship from CONICET. N.S. acknowledges a doctoral research scholarship from Comisión Nacional de Energia Atomica. H.D., P.N.C., G.S.I. and A.W. are permanent researchers of CONICET, Argentina. Fruitful discussions with K. Sugahara on the new adjuvant are gratefully acknowledged.

References

1 L. H. Bookbinder, A. Hofer, M. F. Haller, *et al.* A recombinant human enzyme for enhanced interstitial transport of therapeutics, *J. Controlled Release*, 2006, **114**, 230–241.
2 L. Eikenes, M. Tari, I. Tufto, O. S. Bruland and C. de Lange Davies, Hyaluronidase induces a transcapillary pressure gradient and improves the distribution and uptake of liposomal doxorubicin (Caelyx) in human osteosarcoma xenografts, *Br. J. Cancer*, 2005, **93**, 81–88.
3 I. Muckenschnabel, G. Bernhardt, T. Spruss and A. Buschauer, Hyaluronidase pretreatment produces selective melphalan enrichment in malignant melanoma implanted in nude mice, *Cancer Chemother. Pharmacol.*, 1996, **38**, 88–94.
4 B. P. Toole, Hyaluronan-CD44 Interactions in Cancer: Paradoxes and Possibilities, *Clin. Cancer Res.*, 2009, **15**, 7462–7468.
5 M. A. Jacobetz, D. S. Chan, A. Neesse, *et al.* Hyaluronan impairs vascular function and drug delivery in a mouse model of pancreatic cancer, *Gut*, 2013, **62**, 112–120.
6 H. O. Fadnes, R. K. Reed and K. Aukland, Interstitial fluid pressure in rats measured with a modified wick technique, *Microvasc. Res.*, 1977, **14**, 27–36.
7 C. H. Heldin, K. Rubin, K. Pietras and A. Ostman, High interstitial fluid pressure – an obstacle in cancer therapy, *Nat. Rev. Cancer*, 2004, **4**, 806–813.
8 P. P. Provenzano and S. R. Hingorani, Hyaluronan, fluid pressure, and stromal resistance in pancreas cancer, *Br. J. Cancer*, 2013, **108**, 1–8.
9 E. J. Menzel and C. Farr, Hyaluronidase and its substrate hyaluronan: biochemistry, biological activities and therapeutic uses, *Cancer Lett.*, 1998, **131**, 3–11.
10 S. Sakai, K. Hirano, H. Toyoda, R. J. Linhardt and T. Toida, Matrix assisted laser desorption ionization-time of flight mass spectrometry analysis of hyaluronan oligosaccharides, *Anal. Chim. Acta*, 2007, **593**, 207–213.
11 L. Soltes, G. Kogan, M. Stankovska, *et al.* Degradation of high-molar-mass hyaluronan and characterization of fragments, *Biomacromolecules*, 2007, **8**, 2697–2705.
12 K. Sugahara, S. Yamada, M. Sugiura, *et al.* Identification of the reaction products of the purified hyaluronidase from stonefish (*Synanceja horrida*) venom, *Biochem. J.*, 1992, **283**(Pt 1), 99–104.
13 A. L. Dunn, J. E. Heavner, G. Racz and M. Day, Hyaluronidase: a review of approved formulations, indications and off-label use in chronic pain management, *Expert Opin. Biol. Ther.*, 2010, **10**, 127–131.
14 Hyaluronidase Monograph (Amphadase, Hydase, Vitrase, Hylenex) Final, in: National PBM Drug Monograph, http://www.pbm.va.gov/Clinical%20Guidance/Drug%20Monographs/Hyaluronidase%20Monograph%20(Amphadase,%20Hydase,%20Vitrase,%20Hylenex)%20Final.doc:, VHA Pharmacy Benefits Management Service and the Medical Advisory Panel, Washington, DC, 2008.
15 C. J. Whatcott, H. Han, R. G. Posner, G. Hostetter and D. D. Von Hoff, Targeting the tumor microenvironment in cancer: why hyaluronidase deserves a second look, *Cancer Discovery*, 2011, **1**, 291–296.
16 ClinicalTrials.gov.in, http://www.clinicaltrials.gov/ct2/results?term=PEGPH20&Search=Search:, U.S. National Institutes of Health.
17 C. Brekken and C. de Lange Davies, Hyaluronidase reduces the interstitial fluid pressure in solid tumours in a non-linear concentration-dependent manner, *Cancer Lett.*, 1998, **131**, 65–70.
18 P. P. Provenzano, C. Cuevas, A. E. Chang, V. K. Goel, D. D. Von Hoff and S. R. Hingorani, Enzymatic targeting of the stroma ablates physical barriers to treatment of pancreatic ductal adenocarcinoma, *Cancer cell*, 2012, **21**, 418–429.
19 K. Beckenlehner, S. Bannke, T. Spruss, G. Bernhardt, H. Schonenberg and W. Schiess, Hyaluronidase enhances the activity of adriamycin in breast cancer models *in vitro* and *in vivo*, *J. Cancer Res. Clin. Oncol.*, 1992, **118**, 591–596.
20 S. Guedan, J. J. Rojas, A. Gros, E. Mercade, M. Cascallo and R. Alemany, Hyaluronidase expression by an oncolytic adenovirus enhances its intratumoral spread and suppresses tumor growth, *Mol. Ther.*, 2010, **18**, 1275–1283.
21 S. Ganesh, M. Gonzalez-Edick, D. Gibbons, M. Van Roey and K. Jooss, Intratumoral coadministration of hyaluronidase enzyme and oncolytic adenoviruses enhances virus potency in metastatic tumor models, *Clin. Cancer Res.*, 2008, **14**, 3933–3941.
22 S. Lavilla-Alonso, M. M. Bauer, U. Abo-Ramadan, *et al.* Macrophage metalloelastase (MME) as adjuvant for intratumoral injection of oncolytic adenovirus and its influence on metastases development, *Cancer Gene Ther.*, 2012, **19**, 126–134.
23 C. Brekken, M. H. Hjelstuen, O. S. Bruland and C. de Lange Davies, Hyaluronidase-induced periodic modulation of the interstitial fluid pressure increases selective antibody uptake in human osteosarcoma xenografts, *Anticancer Res.*, 2000, **20**, 3513–3519.
24 M. Gary-Bobo, D. Brevet, N. Benkirane-Jessel, *et al.* Hyaluronic acid-functionalized mesoporous silica nanoparticles for efficient photodynamic therapy of cancer cells, *Photodiagn. Photodyn. Ther.*, 2012, **9**, 256–260.
25 J. M. Rosenholm, V. Mamaeva, C. Sahlgren and M. Linden, Nanoparticles in targeted cancer therapy: mesoporous

 This journal is © The Royal Society of Chemistry 2013

Published on 01 August 2013. Downloaded by Open University on 23/08/2013 18:58:47.

silica nanoparticles entering preclinical development stage, *Nanomedicine*, 2012, **7**, 111–120.
26 G. I. Frost, Recombinant human hyaluronidase (rHuPH20): an enabling platform for subcutaneous drug and fluid administration, *Expert Opin. Drug Delivery*, 2007, **4**, 427–440.
27 W. Stöber, A. Fink and E. Bohn, Controlled growth of monodisperse silica spheres in the micron size range, *J. Colloid Interface Sci.*, 1968, **26**, 62–69.
28 M. Benezra, O. Penate-Medina, P. B. Zanzonico, *et al.* Multimodal silica nanoparticles are effective cancer-targeted probes in a model of human melanoma, *J. Clin. Invest.*, 2011, **121**, 2768–2780.
29 G. Durgun, K. Ocakoglu and S. Ozcelik, Systematic Tuning the Hydrodynamic Diameter of Uniformed Fluorescent Silica Nanoparticles, *J. Phys. Chem. C*, 2011, **115**, 16322–16332.
30 G. Decher, Fuzzy Nanoassemblies: Toward Layered Polymeric Multicomposites, *Science*, 1997, **277**, 1232–1237.
31 F. Caruso, H. Lichtenfeld, E. Donath and H. Möhwald, Investigation of Electrostatic Interactions in Polyelectrolyte Multilayer Films: Binding of Anionic Fluorescent Probes to Layers Assembled onto Colloids, *Macromolecules*, 1999, **32**, 2317–2328.
32 P. Scodeller, R. Carballo, R. Szamocki, L. Levin, F. Forchiassin and E. J. Calvo, Layer-by-layer self-assembled osmium polymer-mediated laccase oxygen cathodes for biofuel cells: the role of hydrogen peroxide, *J. Am. Chem. Soc.*, 2010, **132**, 11132–11140.
33 P. Scodeller, V. Flexer, R. Szamocki, *et al.* Wired-enzyme core–shell Au nanoparticle biosensor, *J. Am. Chem. Soc.*, 2008, **130**, 12690–12697.
34 V. Flexer, E. S. Forzani, E. J. Calvo, S. J. Luduena and L. I. Pietrasanta, Structure and thickness dependence of "molecular wiring" in nanostructured enzyme multilayers, *Anal. Chem.*, 2006, **78**, 399–407.
35 M. W. Li, A. I. Yudin, K. R. Robertson, G. N. Cherr and J. W. Overstreet, Importance of glycosylation and disulfide bonds in hyaluronidase activity of macaque sperm surface PH-20, *J. Androl.*, 2002, **23**, 211–219.
36 F. Caruso and C. Schüler, Enzyme Multilayers on Colloid Particles: Assembly, Stability, and Enzymatic Activity, *Langmuir*, 2000, **16**, 9595–9603.
37 W. Schärtl, *Light Scattering from Polymer Solutions and Nanoparticle Dispersions*, Springer, New York, 2007.
38 D. S. Monteiro, T. M. Nobre and M. E. Zaniquelli, Hyaluronidase behavior at the air/liquid and air/lipid interfaces and improved enzymatic activity by its immobilization in a biomembrane model, *J. Phys. Chem. B*, 2011, **115**, 4801–4809.
39 E. A. Turley and M. Tretiak, Glycosaminoglycan production by murine melanoma variants *in vivo* and *in vitro*, *Cancer Res.*, 1985, **45**, 5098–5105.
40 H. Meng, M. Liong, T. Xia, *et al.* Engineered design of mesoporous silica nanoparticles to deliver doxorubicin and P-glycoprotein siRNA to overcome drug resistance in a cancer cell line, *ACS Nano*, 2010, **4**, 4539–4550.
41 A. Baeza, E. Guisasola, E. Ruiz-Hernández and M. Vallet-Regí, Magnetically Triggered Multidrug Release by Hybrid Mesoporous Silica Nanoparticles, *Chem. Mater.*, 2012, **24**, 517–524.
42 S. R. Hingorani, W. P. Harris, J. T. Beck, *et al.* A phase Ib study of gemcitabine plus PEGPH20 (pegylated recombinant human hyaluronidase) in patients with stage IV previously untreated pancreatic cancer. In: 2013 American Society of Clinical Oncology Annual Meeting, Chicago, IL, *J. Clin. Oncol.*, 2013, **31**(suppl. 4010).
43 Sigma-Aldrich. Enzymatic Assay of Hyaluronidase, http://www.sigmaaldrich.com/technical-documents/protocols/biology/enzymatic-assay-of-hyaluronidase.html.